Article

Late-stage oxidative C(sp^3)–H methylation

https://doi.org/10.1038/s41586-020-2137-8

Received: 6 December 2019

Accepted: 5 March 2020

Published online: 16 March 2020

Check for updates

Kaibo Feng[1,4], Raundi E. Quevedo[1,4], Jeffrey T. Kohrt[2], Martins S. Oderinde[3], Usa Reilly[2] & M. Christina White[1]✉

Frequently referred to as the 'magic methyl effect', the installation of methyl groups—especially adjacent (α) to heteroatoms—has been shown to dramatically increase the potency of biologically active molecules[1–3]. However, existing methylation methods show limited scope and have not been demonstrated in complex settings[1]. Here we report a regioselective and chemoselective oxidative C(sp^3)–H methylation method that is compatible with late-stage functionalization of drug scaffolds and natural products. This combines a highly site-selective and chemoselective C–H hydroxylation with a mild, functional-group-tolerant methylation. Using a small-molecule manganese catalyst, Mn(CF_3PDP), at low loading (at a substrate/catalyst ratio of 200) affords targeted C–H hydroxylation on heterocyclic cores, while preserving electron-neutral and electron-rich aryls. Fluorine- or Lewis-acid-assisted formation of reactive iminium or oxonium intermediates enables the use of a mildly nucleophilic organoaluminium methylating reagent that preserves other electrophilic functionalities on the substrate. We show this late-stage C(sp^3)–H methylation on 41 substrates housing 16 different medicinally important cores that include electron-rich aryls, heterocycles, carbonyls and amines. Eighteen pharmacologically relevant molecules with competing sites—including drugs (for example, tedizolid) and natural products—are methylated site-selectively at the most electron rich, least sterically hindered position. We demonstrate the syntheses of two magic methyl substrates—an inverse agonist for the nuclear receptor RORc and an antagonist of the sphingosine-1-phosphate receptor-1—via late-stage methylation from the drug or its advanced precursor. We also show a remote methylation of the B-ring carbocycle of an abiraterone analogue. The ability to methylate such complex molecules at late stages will reduce synthetic effort and thereby expedite broader exploration of the magic methyl effect in pursuit of new small-molecule therapeutics and chemical probes.

The introduction of methyl groups has the potential to dramatically improve the biological activities of a drug candidate by altering its binding affinity, solubility and metabolism[1–8]. Such changes have been demonstrated to increase the potency of lead compounds more than 2,000-fold and to enable interrogation of biological processes[6–8] (Fig. 1a). Although methyl groups are ubiquitous in small-molecule drugs[1], no general method is available to incorporate them into complex molecules at late stages. Accordingly, de novo synthesis—a rate-limiting step in drug discovery that impairs its overall atom economy—is required[9,10]. A practical synthetic method that allows selective installation of methyl groups from C–H bonds at sites adjacent to heteroatoms, where the magic methyl effect is often most substantial, would streamline the diversification of drug leads and encourage more comprehensive investigations of this effect. Over the past decade, considerable progress has been made in developing C(sp^3)–H alkylation methods in which the N- or O-heterocycle acts as a nucleophilic coupling partner[11–17]. Such cross-couplings have shown broad scope with respect to alkyl electrophiles, but limited scope of the metallated heterocyclic intermediates generated via substrate-controlled deprotonation or single-electron transfer (SET). Cases demonstrated with methyl electrophiles have focused on simple azacycles[11,13,15–17]. Expanding the heterocyclic scope to include dissymmetric substrates, epimerizable stereocentres, electrophilic functionalities (for example, carbonyl and nitrile), remote basic amines, heteroaromatics and halogenated aromatics remains a major challenge to be overcome for widespread use in late-stage diversification. In addition, although direct C–C bond forming reactions may be desirable for installing larger and/or functionalized alkyl groups, direct methylation often results in inseparable mixtures with the starting material owing to the small size and electron neutrality of the methyl group.

We sought to approach C(sp^3)–H methylation in N- and O-containing heterocycles in an oxidative fashion through a hydroxylated intermediate, with subsequent iminium or oxonium ion formation and methylation (Fig. 1b). Catalyst control could be leveraged to influence the site-selectivity and chemoselectivity of C–H hydroxylation in a broad range of heterocycles (Fig. 1c, d). Reports of alkylations of

[1]Department of Chemistry, Roger Adams Laboratory, University of Illinois, Urbana, IL, USA. [2]Pfizer Worldwide Research and Development, Groton Laboratories, Groton, CT, USA. [3]Research and Development, Bristol-Myers Squibb Company, Lawrenceville, NJ, USA. [4]These authors contributed equally: Kaibo Feng, Raundi E. Quevedo. ✉e-mail: mcwhite7@illinois.edu

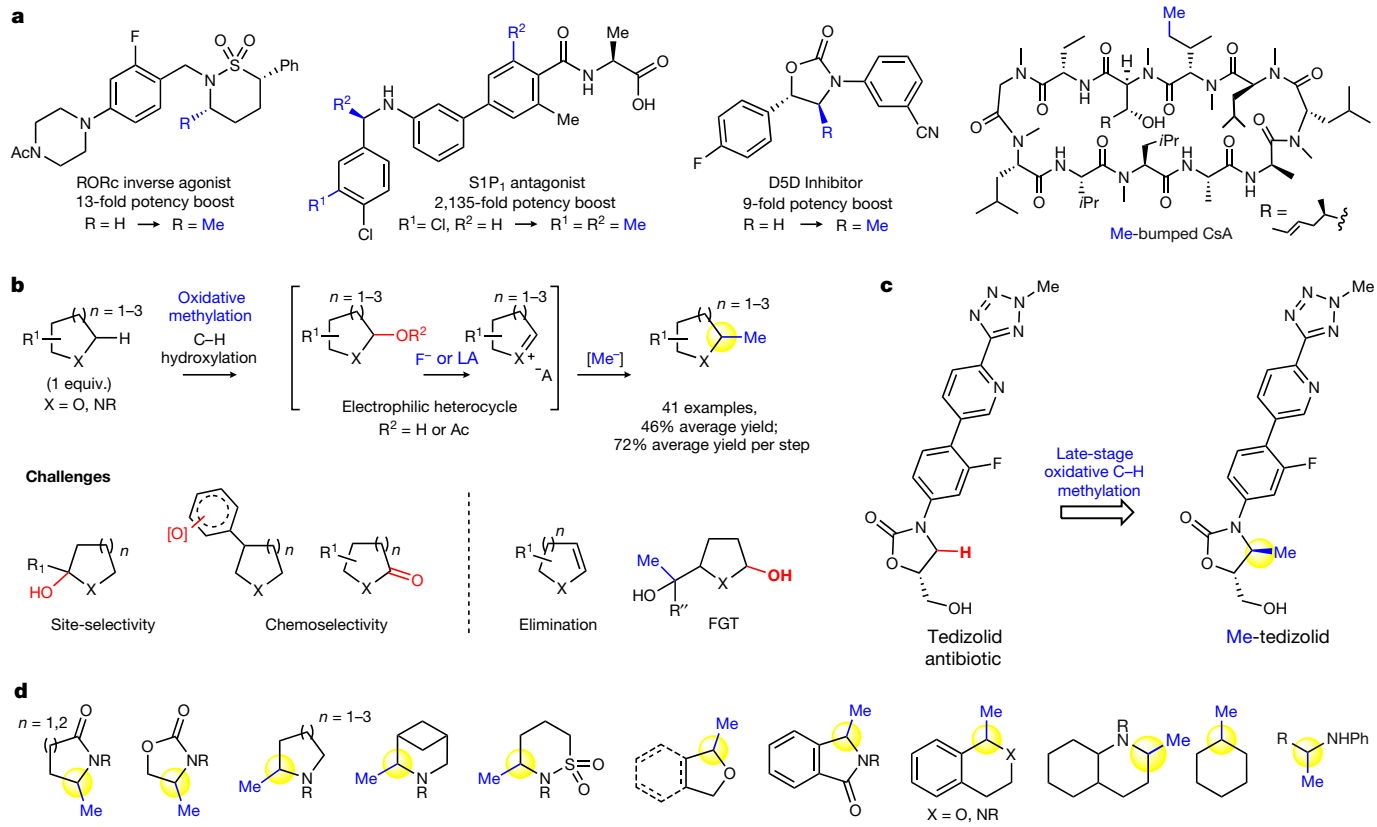

Fig. 1 | C(sp^3)–H methylation. a, The magic methyl effect boosts the potency of drugs (such as RORc, $S1P_1$ and Δ−5 desaturase (D5D)) and furnishes biological probes (such as cyclosporin A (CsA)). **b**, Top row, this oxidative methylation proceeds through an electrophilic intermediate. Bottom row, challenges include unselective oxidation and overoxidation (see site-selectivity and chemoselectivity), as well as elimination and unselective methylation pathways (see functional group tolerance (FGT)). **c**, Late-stage oxidative methylation of the antibiotic tedizolid. **d**, We have demonstrated this oxidative C–H methylation on 16 different pharmaceutically relevant cores. Using one equivalent of substrate, methylation proceeds site-selectively and with functional group tolerance to afford preparative yields in 41 examples (including 18 complex bioactive molecules).

N-acyliminium ions are of limited scope[18,19]. Although C(sp^3)–H oxidation α to heteroatoms has been well demonstrated, substrate-controlled selectivities can afford poor site- and chemoselectivity, thereby limiting examples in complex settings[20]. Moreover, the strong hyperconjugative activation of hemiaminals and hemiacetals typically promotes overoxidation to the corresponding carbonyl, calling for reduction before or after methylation (Fig. 1b)[21–26].

The catalyst $Mn(CF_3PDP)(MeCN)_2(SbF_6)_2$ (**1**) (where CF_3PDP is 1,1′-bis((5-(2,6-bis(trifluoromethyl)phenyl)pyridin-2-yl)methyl)-2,2′-bipyrrolidine) has been reported to uniquely control site- and chemoselectivity in hydroxylating strong methylene C(sp^3)–H bonds while tolerating halogenated arenes, although the tolerance for electron-neutral or electron-rich aromatic and some heteroaromatic rings remained a challenge[27] (Fig. 1b). We questioned whether sterically hindered catalyst **1** could result in faster C–H hydroxylation than alcohol oxidation for hyperconjugatively activated C–H bonds, and whether under milder oxidation conditions such a rate difference would increase chemoselectivity and yield for the hydroxylated product. Under the previously reported forcing conditions (10 mol% **1**, 5 equiv. H_2O_2)[27], oxidation of arylated γ-lactam (**2**) afforded a substantial amount of overoxidation to the corresponding imide (Fig. 2a, **4b**, 41%). Lowering the catalyst and hydrogen peroxide loadings (to 0.5 mol% **1**, 2.0 equiv. H_2O_2) enabled the C–H bond α to nitrogen (α-N) to be hydroxylated to hemiaminal intermediates (hemiaminal, and hemiaminal acetate from AcOH) with an excellent yield of 82% (**4a**). Consistent with slower alcohol oxidation, exposure of alcohol **4a** to identical oxidation conditions afforded 84% hemiaminals with only 10% imide **4b** (Fig. 2b). By contrast, exposure of alcohol **4a** to the forcing conditions afforded predominantly imide **4b** (54%) with only 17% hemiaminals. Under mild oxidation conditions, we also observed enhanced chemoselectivities for electron-rich and electron-neutral aromatics and heteroaromatics, probably because of attenuation of similarly higher-energy overoxidation pathways (vide infra). Notably, this constitutes among the highest substrate/catalyst ratios (S/C = 200) reported so far for a preparative C(sp^3)–H hydroxylation reaction in a complex setting. The ability to separate the hydroxylated intermediate before methylation, while not necessary for alkylation, avoids the formation of an inseparable mixture of the methylated product and starting material, often observed in direct methylation[17]. As expected, Fe(PDP) and $Fe(CF_3PDP)$—used previously for oxidative α-arylation of aliphatic peptides[28–30]—gave a complex mixture of aromatic oxidation products (Extended Data Table 1). Mn(PDP), shown to hydroxylate simple linear amides[31], was not reactive enough to promote preparative hydroxylation of **2**, but can be uniquely effective for some sterically hindered substrates (vide infra).

A further challenge with an oxidative methylation approach was to identify a way to activate the hemiaminal/hemiacetal towards attack by a nucleophilic methyl source without resulting in either undesirable elimination to the enamine, or attack at other electrophilic moieties in complex substrates (Fig. 1b). The modestly nucleophilic and Lewis acidic nature of organoaluminium reagents suggested that they could achieve such selective reactivity. Their high affinity for fluorine, coupled with their tolerance of Lewis acids, afforded a means of generating reactive iminium or oxonium species from transient C–F or from C–OH bond ionization[32,33]. High functional-group tolerance was also expected, given the ability of organoaluminium reagents to methylate oxoniums at late stages in the presence of other electrophilic functionalities[34].

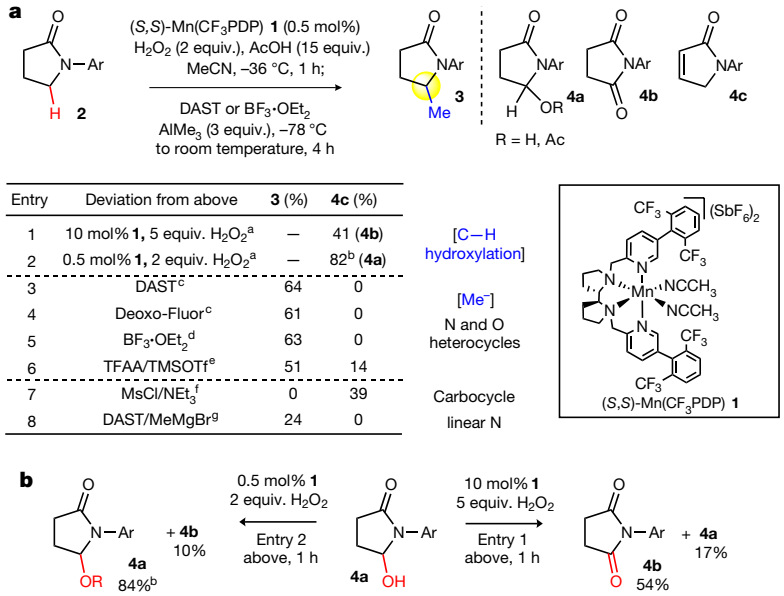

Entry	Deviation from above	3 (%)	4c (%)
1	10 mol% **1**, 5 equiv. H_2O_2[a]	—	41 (**4b**)
2	0.5 mol% **1**, 2 equiv. H_2O_2[a]	—	82[b] (**4a**)
3	DAST[c]	64	0
4	Deoxo-Fluor[c]	61	0
5	$BF_3{\cdot}OEt_2$[d]	63	0
6	TFAA/TMSOTf[e]	51	14
7	MsCl/NEt_3[f]	0	39
8	DAST/MeMgBr[g]	24	0

Fig. 2 | Reaction development. a, Optimization of the oxidative methylation reaction. Note that for achiral substrates, catalysts (*R*,*R*)-**1** and (*S*,*S*)-**1** can be used interchangeably. DAST or $BF_3{\cdot}OEt_2$ was generally used as the hydroxyl activator, with trimethylaluminium as the methyl source. Isolated yields are based on the average of two to three experiments. Ar = *p*-Cl(C_6H_4). **b**, Exposure of hemiaminal (**4a**) to mild C–H hydroxylation (0.5 mol% **1**, 2 equiv. H_2O_2), developed herein, produces little overoxidation to the imide. The previous forcing condition (10 mol% **1**, 5 equiv. H_2O_2) results in imide as the major product. [a]No methylation. [b]Mixture of hemiaminal (64–71%) and hemiaminal acetate (13–18%) from AcOH. [c]1 equiv. [d]2 equiv. [e]TFAA, 1 equiv.; TMSOTf, 1 equiv. [f]MsCl, 1 equiv.; NEt_3, 1 equiv.; $NaHCO_3$ wash; $AlMe_3$, 3 equiv.; –78 °C, 2 h; room temperature, 1 h. [g]MeMgBr, 3 equiv.; –78 °C, 3 h.

After substantial experimentation (shown in abbreviated fashion in Fig. 2a), we arrived at a scalable general procedure using either diethylaminosulfur trifluoride (DAST) or boron trifluoride diethyl etherate ($BF_3{\cdot}OEt_2$) as the hydroxyl activator for iminium formation, with $AlMe_3$ as an inexpensive, commercial methylating reagent. Thermally stable bis(2-methoxyethyl)aminosulfur trifluoride (Deoxo-Fluor) could also be used. In general, the fluorine-assisted methylation strategy should be used in substrates containing Lewis basic or electrophilic functional groups, whereas those lacking such functionality can be methylated via the BF_3 activation strategy (Extended Data Table 1). When unreacted hemiaminal acetate is observed, esterification of the hemiaminal by trifluoroacetic anhydride (TFAA) and subsequent activation of both esters with trimethylsilyl triflate (TMSOTf) to furnish the iminium can be used[34]. The ability to vary the ionization method with $AlMe_3$ is essential to the broad scope of this methylation, providing a facile handle to tune reactivity and/or selectivity for a given substrate in cases in which unreacted hemiaminal intermediates or enamine byproducts are observed (vide infra).

We examined alternative activation modes with $AlMe_3$ and other methylating reagents with DAST (Extended Data Table 1). In hemiaminals, base-mediated formation of an activated C–O bond (that is, mesylation) led predominantly to elimination (Fig. 2a). Grignard reagents, even at cryogenic temperatures, afford diminished yields relative to $AlMe_3$, probably because of poor functional-group tolerance. Although ineffective for the methylation of heterocyclic substrates, these reagents can be used to effect methylation in challenging linear secondary amine and carbocyclic substrates (vide infra; **51**, **53**).

We explored oxidative methylation for its capacity to methylate a collection of 22 compounds comprising 10 different heterocyclic cores commonly found in pharmaceuticals (Fig. 3). We successfully carried out a gram-scale methylation of **2** in 71% yield via DAST activation; an ethyl group could also be installed using commercial triethylaluminium (**5**, 51%). Methylated δ-lactam **6** was isolated in 58% yield; analogous to the γ-lactam, under more forcing oxidation conditions δ-lactam gave predominantly imide (60%). For amide **2**, methylated **3** was observed in preparative yields with both DAST and BF_3 ionization (Fig. 2a). However, in oxazolidinones, housing more labile carbonyls, fluorination with DAST furnished substantially higher yields (**7**, 55% versus 10% with BF_3; Extended Data Table 1; **8**, 63%). Pyrrolidine, the fifth most common nitrogen heterocycle in drugs[35,36], undergoes hydroxylation with no substantial overoxidation to pyrrolidinone, followed by BF_3-promoted methylation to afford monomethylated product **9** in 54% yield. Essential for late-stage derivatization and orthogonal to most radical processes, high site-selectivity for methylation at the less sterically hindered methylene site was observed in substrates bearing more activated tertiary (3°) aliphatic, 3° benzylic, and 3° α-carbonyl C–H bonds to afford products in preparative yields (**10**–**13**). Full stereoretention was measured with chiral substrates leading to **12** and **13**, indicating that the high regioselectivity can be attributed to catalyst control of Mn(CF_3PDP) **1** in the C–H cleavage step. Methyl ester, ketone, acetate and nitrile—not well tolerated with strongly nucleophilic methylation reagents—were maintained using DAST activation/$AlMe_3$ methylation (**12**–**15**). Methylation on a 3-phenylpyrrolidine derivative proceeded regioselectively at the methylene site distal from the phenyl group, furnishing the 5-methylated product **16** in useful yield. Such chemoselectivity for electron-neutral aromatics has not been previously demonstrated: at higher catalyst loadings, **1** afforded poor yields and chemoselectivities[27].

In piperidines—the most common nitrogen heterocycle in small-molecule drugs[35,36]—both DAST and BF_3 activation should be tried: enamine formation competes strongly with methylation and depends highly on both the substrate and the mode of hemiaminal activation (Fig. 3). For example, a pipecolic acid derivative gave 2% of the methylated product with 60% enamine byproduct under DAST activation, whereas the BF_3 activation furnished **17** in 47% overall yield. Alternatively, methylation of piperidinyl-2-methyl acetate using BF_3 did not fully convert the hemiaminal to methylated product, whereas DAST activation afforded **18** in 64% yield. Gamma-substituted piperidines are prevalent structures in drugs, such as in paliperidone and paroxetine. An *N*-nosyl intermediate in the synthesis of paliperidone was selectively methylated using the DAST protocol to give **19** in 37% yield with no protection of the benzisoxazole ring γ to nitrogen. However, methylation

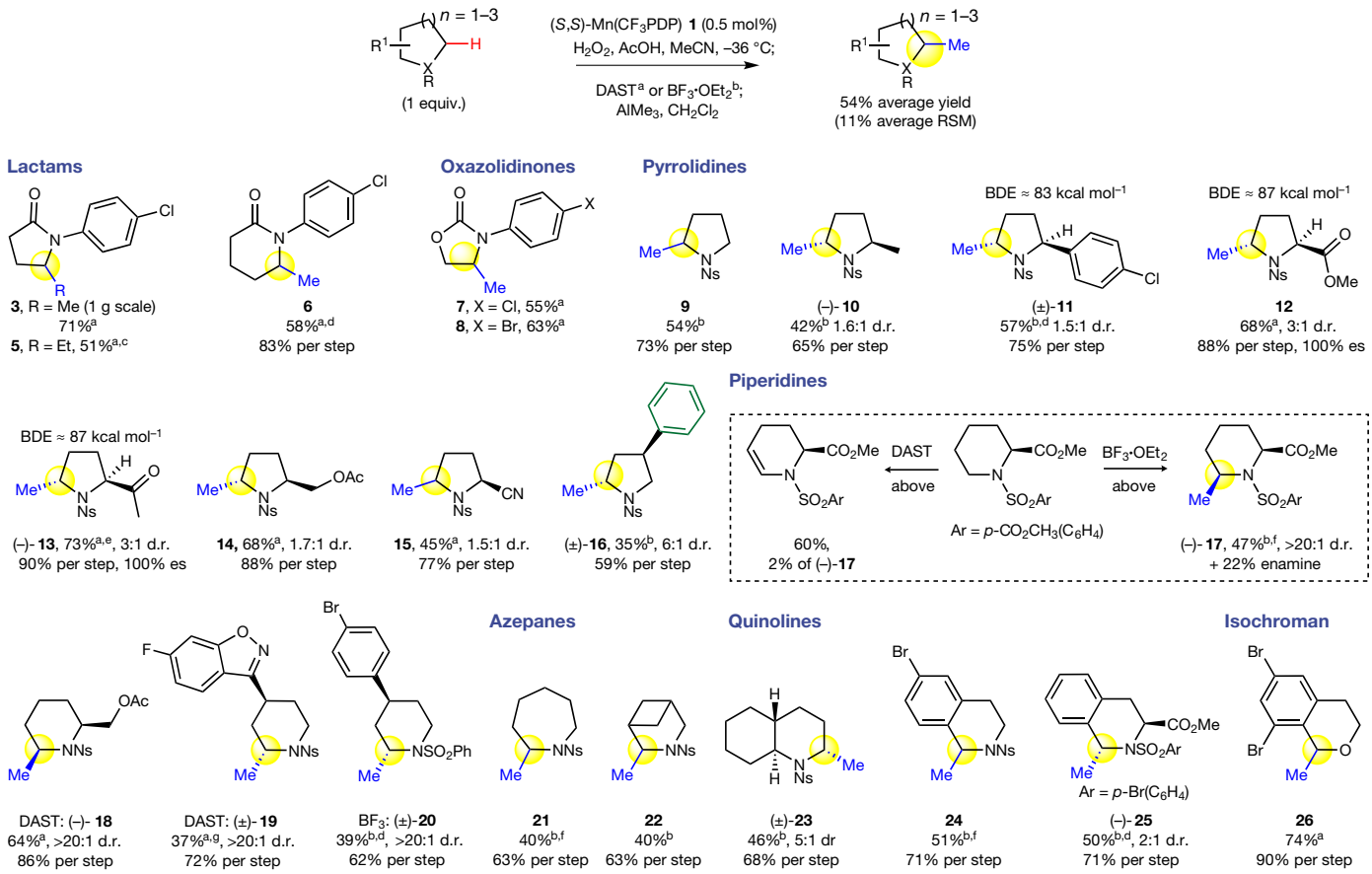

Fig. 3 | Ten different heterocyclic cores, commonly found in pharmaceuticals, explored in the Mn(CF$_3$PDP) (1)-catalysed C–H oxidative methylation. Twenty-two heterocycles—including lactams, oxazolidinones, pyrrolidines, piperidines, azepane, azabicycloheptane, quinolines and isochroman—were oxidatively methylated in preparative overall yields (54% average) using limiting substrate. es, enantiospecificity; RSM, recovered starting material. Isolated yields are based on the average of three experiments. General oxidation: substrate (1 equiv.), catalyst (0.5 mol%), AcOH in MeCN, –36 °C; H_2O_2 (2 or 5 equiv.) in MeCN syringe pump for 1 h. Mixture passed through silica plug, EtOAc flush, concentrated before isolation or methylation. For insoluble substrates, CH_2Cl_2 was added to MeCN and/or the temperature of the oxidation reaction was increased to 0 °C. [a]DAST activation: crude in CH_2Cl_2 (0.2 M), DAST (1 equiv.) added at –78 °C; room temperature (rt) for 1 h; cooled to –78 °C, $AlMe_3$ added, stirred 2 h; rt for 1 h. [b]BF_3 activation: crude in CH_2Cl_2 (0.2 M), –78 °C, $AlMe_3$ (3 equiv.) and BF_3·OEt_2 (2 equiv.) sequentially added, stirred 1 h; rt for 3 h. [c]Triethylaluminium. [d]2 mol% (*S*,*S*)-**1**. [e]$AlMe_3$ –78 °C, 3 h. [f]1 mol% (*S*,*S*)-**1**. [g]For facile purification, hemiaminal isolated before methylation. 10 mol% (*S*,*S*)-**1**, rt, starting material recycled once.

of γ-(4-bromophenyl)piperidine with DAST resulted predominantly in enamine formation, whereas the BF_3 activation strategy afforded 39% yield of methylated **20**. Notably, all piperidines furnished a single observed methylated diastereomer, probably as a result of the rigid half-chair conformation of the iminium intermediate[37].

Other simple cyclic amines—such as azepane, azabicycloheptane and decahydroquinoline—were selectively methylated using the BF_3 activation protocol α-N to afford 40–46% overall yields of mono-methylated products **21**–**23**. Tetrahydroisoquinoline, among the top 20 nitrogen heterocycles in drugs[36], was oxidatively methylated using BF_3 activation in good yields for both a brominated and an unsubstituted aromatic structure (**24**, 51%; **25**, 50%), with lower yields observed using DAST activation. In contrast with most radical-based oxidation methods that oxidize isochromans to isochromanones, using Mn(CF$_3$PDP) **1**, little overoxidation was observed. 6,8-Dibromoisochroman was oxidatively methylated using DAST/$AlMe_3$ in 74% yield (**26**); BF_3 activation for these types of oxygen heterocycles afforded ring-opening products[38].

We explored the ability of highly site- and chemoselective C–H hydroxylation catalysed by Mn(CF$_3$PDP) **1**, coupled to a Lewis-acid/fluorine-promoted methylation, to provide a general method for installing methyl groups directly into the hydrocarbon cores of complex, bioactive molecules, thereby avoiding lengthy and costly de novo synthesis[1,9,10] (Fig. 4). Acetylated cromakalim—a potassium channel activator housing a γ-lactam with tertiary and secondary hyperconjugatively activated α-N C(sp^3)–H bonds—underwent oxidative methylation at the less activated but more sterically accessible secondary site in good yield (**27**, 51%). The acetate could be readily removed to furnish methylated cromakalim **28** in 85% yield. The methyl ester of indoprofen, an anti-inflammatory drug investigated for spinal muscular atrophy[39], was oxidatively methylated at its central isoindolinone core in synthetically useful yields (**29**, 33%). The enhanced chemoselectivity of oxidative methylation with **1** under reduced loadings is evident when comparing with results at higher loadings (10 mol%), in which **29** was obtained in diminished yields (7%) owing to poor chemoselectivity. Chloroindoprofen methyl ester—a derivative with decreased electron density on the aromatic ring—underwent oxidative methylation in higher yields (**30**, 55%).

Fenspiride, an antitussive drug, was oxidatively methylated in a useful overall yield (**31**, 24%) at a methylene site adjacent to the quaternary centre of an unprotected spiro-oxazolidinone, using the (*S*,*S*)-Mn(PDP)$(SbF_6)_2$ catalyst that is less sensitive to sterics[27]. The basic piperidine nitrogen of fenspiride was protected with HBF_4 and rendered a strong electron-withdrawing group, deactivating a distal benzylic site and three α-N sites towards C–H oxidation[40]. Notably, SET reactions proceeding via basic amine catalysis (for example, quinuclidine) are not generally amenable to this kind of nitrogen-protection strategy and

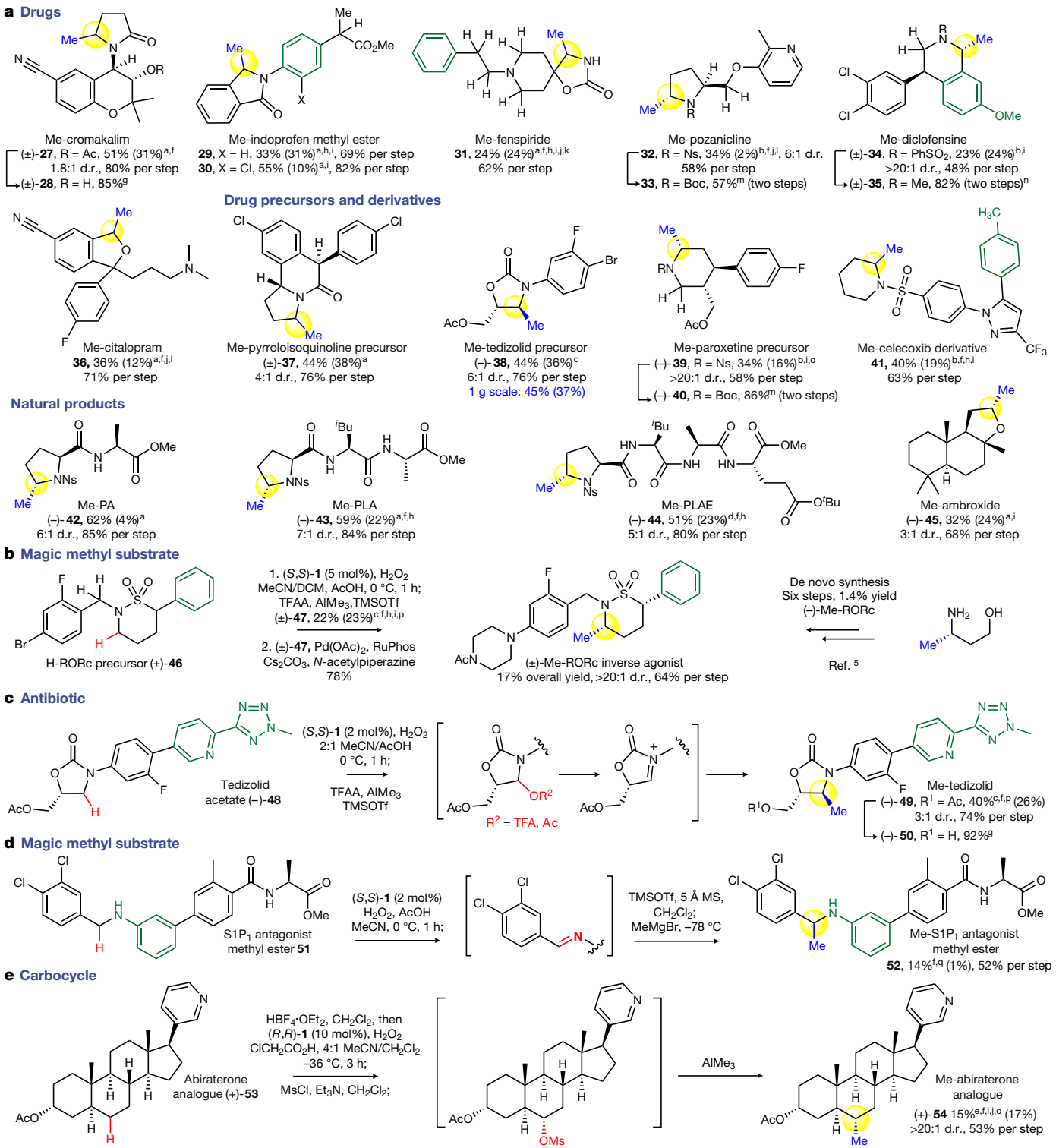

Fig. 4 | Application of oxidative methylation for late-stage functionalization. **a**, Selective methylation of drugs, drug precursors, intermediates and natural products underscores the power of this method for late-stage applications. Generally, 0.5–5 mol% (*S*,*S*)-**1** and 2 or 5 equiv. H_2O_2 were used for oxidation. Higher catalyst and oxidant loadings were applied when conversions were low. Isolated yields are based on the average of three experiments. Explicit C–H bonds denote competing sites of oxidation (for example, Me-fenspiride). Green colouring denotes oxidatively labile aromatic groups (for example, Me-diclofensine). **b**, Methylation of an RORc inverse agonist precursor rapidly furnishes the analogue with a 13-fold boost in potency. Details of synthesis from (*S*)-3-aminobutan-1-ol are from ref. [5]. **c**, Methylation of the antibiotic tedizolid acetate furnishes Me-tedizolid. **d**, Methylation of linear aniline in the $S1P_1$ antagonist methyl ester occurs at a position where the magic methyl effect was observed to contribute to a 2,135-fold potency boost (see ref. [6]). **e**, Remote methylation of a carbocycle on an abiraterone analogue. [a]DAST activation. [b]BF_3 activation. [c]TMSOTf activation: TFAA, rt, 1 h; cooled to −78 °C, $AlMe_3$ and TMSOTf sequentially added, 2 h; then rt, 1 h. [d]Deoxo-Fluor activation. [e]Mesylation activation: MsCl and Et_3N added, rt, 1 h; $NaHCO_3$ wash, dried, condensed; redissolved in CH_2Cl_2, $AlMe_3$ added at −78 °C, stirred 2 h; then rt, 1 h. [f]Oxidation intermediates isolated before methylation. [g]1 M NaOH/MeOH. [h]Starting material recycled once. In some cases, isolated yields are based on an average of two experiments; see Supplementary Information. [i]For insoluble substrates, CH_2Cl_2 was added to MeCN and/or the temperature of the oxidation reaction was increased to 0 °C. [j]HBF_4 protection (see ref. [40]). [k]10 mol% (*S*,*S*)-Mn(PDP)$(SbF_6)_2$. [l]10 mol% (*S*,*S*)-**1**. [m]PhSH, Cs_2CO_3; Boc_2O. [n]Mg, NH_4Cl; formaldehyde, formic acid. [o]10 mol% (*R*,*R*)-**1**. [p]2 equiv. TMSOTf. [q]TMSOTf (1.2 equiv.), 0 °C, 1 h, then MeMgBr (3.0 equiv.) −78 °C, 4 h, repeated once.

therefore do not undergo remote C–H functionalizations[17,24]. A derivative of pozanicline—a neuroprotective drug evaluated for the treatment of attention deficit hyperactivity disorder (ADHD)[41]—undergoes α-N oxidative methylation at the pyrrolidine in useful yield and diastereoselectivity (**32**, 34%, diastereomeric ratio (d.r.) 6:1). The HBF_4 protection deactivates the basic pyridine moiety and its proximal ethereal sites from oxidation with **1**. Although DAST activation produced similar yields, a higher diastereoselectivity was obtained with BF_3 activation (6:1 compared with 3:1), possibly because of different iminium counterions (Fig. 1b). The nosyl (Ns) group on pyrrolidine, a convenient chromophoric protecting group for secondary amines, was readily removed using thiophenol and subsequently protected with tert-butyloxycarbonyl (Boc) to afford **33** in 57% overall yield. Underscoring the unique chemoselectivity of this method, a derivative of the antidepressant diclofensine was oxidatively methylated at its tetrahydroisoquinoline core to afford **34** in useful yield despite the presence of a very electron-rich methoxyphenyl. Mild, reductive desulfonation followed by reductive amination furnished methyl-diclofensine **35** in 82% yield. The antidepressant drug citalopram, upon HBF_4 protection of the tertiary amine, is oxidatively methylated at its dihydroisobenzofuran core to afford **36**. DAST activation was used for most of these densely functionalized substrates, whereas BF_3 activation was more effective for the tetrahydroisoquinoline core.

A precursor to pyrroloisoquinoline—a prevalent structure in compounds with neurotransmitter-uptake-inhibitory properties[42]—undergoes selective oxidative methylation at the less sterically hindered methylene site, versus the more activated tertiary, benzylic sites, to furnish **37** (44% yield, Fig. 4a). Oxidation of a carbamate precursor to the antibiotic tedizolid furnished substantial amounts of hemiaminal acetate that could be methylated in a useful overall yield under TFAA/TMSOTf-assisted methylation (**38**, 44%). This method is operationally facile and can be performed on a gram scale with no loss in efficiency (45% yield). Fluorination afforded lower yields of methylated product **38** owing to unconverted hemiaminal acetate. The core piperidine of a paroxetine precursor and metabolite[43] was oxidatively methylated in useful overall yields (**39**, 34%) preferentially at the less sterically hindered methylene site remote from the 3-acetoxymethyl group. Nosyl deprotection and subsequent Boc protection afforded **40** in 86% yield. A piperidine derivative of the anti-inflammatory drug celecoxib was mono-methylated to afford **41** in good overall yield in the presence of an oxidatively labile tolyl group and pyrazole, both tolerated during C–H oxidation with **1** and requiring no protection. In these piperidine substrates, BF_3 activation was effective in furnishing methylated products.

Methylation of proline-based di-, tri-, and tetrapeptides proceeded with good overall yields and mass balances (**42**, **43**, **44**) with **1** under fluorine-assisted oxidative methylation conditions (Fig. 4a). Deoxo-Fluor may be used in substrates such as that of tetrapeptide **44**, for which isolation from the polar byproducts of DAST is challenging. Although effective in promoting the arylation of peptides with electron-rich aromatic nucleophiles, BF_3 activation in the $AlMe_3$ methylation of peptides afforded complex mixtures, probably arising from activation of the amide carbonyls[30]. Ambroxide, a naturally occurring terpenoid, also underwent selective oxidative methylation using DAST at a methylene site α to oxygen on its tetrahydrofuran ring, affording **45** in 32% yield (and 19% of sclareolide lactone). The use of BF_3 in this case promoted ring opening. Notably, Fe(PDP), ruthenium-mediated oxidation and **1** under forcing conditions all afforded sclareolide lactone as the major product isolated (see Supplementary Information)[10,21,28].

The sultam ring in **46**—an advanced intermediate of an RORc inverse agonist (Fig. 4b)—was oxidatively methylated with **1**, using TFAA/TMSOTf activation with $AlMe_3$, to afford **47** as the *syn*-diastereomer. Other activation modes, such as BF_3, resulted in deleterious elimination pathways. Notably, an oxidatively labile phenyl moiety and a doubly activated benzylic methylene site were tolerated. Previous installation of the *syn*-methyl group afforded a 13-fold increase in potency relative to the unmethylated version in an assay for the interaction between RORc and the steroid receptor coactivator 1 (SRC1); however, it required a six-step de novo synthesis, resulting in a 1.4% overall yield[5]. This analogue and others are now accessible via cross-coupling with methylated intermediate **47**.

Tedizolid, a commercial oxazolidinone antibiotic for acute bacterial skin infections, bears numerous oxidatively sensitive functional groups such as pyridine, tetrazole and *N*-methyl (Fig. 4c). Oxidation by $Mn(CF_3PDP)$ **1** (2 mol%) of tedizolid acetate **48** proceeded in approximately 53% yield of oxidized products (3:1 hemiaminal:acetate) with no protection of the dense nitrogen functionalities. The major challenge was to identify a procedure to install the methyl group from the hemiaminal intermediates. Activation via fluorination furnished primarily eliminated products not observed on the simpler core structure (**38**, Fig. 4a), whereas BF_3 activation resulted in side reactions. However, under TFAA/TMSOTf activation, elimination was suppressed and the methylated product **49** was obtained in a 40% overall yield (74% per step), comparable to that of the simpler precursor **38**. Deprotection of the acetate in 92% yield afforded methyl-tedizolid **50**, an interesting candidate for future biological evaluation given that a ninefold boost in potency has been reported for similar oxazolidinone cores with methylation at the same position[44] (Fig. 1a).

We questioned whether the scope of this reaction could be extended beyond heterocycles, and found that oxidative C–H methylation is not restricted to substrates that can form iminium or oxonium intermediates: promising reactivity has been observed for both imines and remote alcohols generated via C–H hydroxylation with **1**. An antagonist of the sphingosine-1-phosphate receptor-1 ($S1P_1$), the benzylic and aromatic methylations of which afforded a 2,135-fold increase in potency[6], was methylated in its methyl ester form (**51**, Fig. 4d). Although oxidation of the antagonist was successful without the need for protection of the aniline motif, the resulting imine was much less reactive than an iminium and required a stronger nucleophile than $AlMe_3$. In this case, we found that methylmagnesium bromide at cryogenic temperatures—with TMSOTf activation of the imine—produced the methylated product without eroding the amide and ester functional groups (**52**, 14%, 52% per step).

At higher catalyst loadings, $Mn(CF_3PDP)$ **1** is an effective catalyst for methylene C–H bond hydroxylations[27]. Abiraterone analogue **53** was hydroxylated in approximately 32% yield (with 16% ketone) in one step, without recycling the starting material as required in $Fe(CF_3PDP)$ catalysis[40] (Fig. 4e). In carbocyclic substrates, displacement of a C–F bond or ionization with a Lewis acid is difficult; however, mesylates of such aliphatic alcohols are stable and can be activated by $AlMe_3$ to undergo substitution[45]. By replacing fluorination with mesylation, **53** was successfully methylated as a single observed diastereomer (**54**, 15% overall yield, 53% per step), probably through a carbocation intermediate. To the best of our knowledge, this is the first method that enables such remote methylation at unactivated $C(sp^3)$–H bonds. The discovery of this reactivity underscores the importance of developing methylene oxidations that afford predominantly alcohol products.

Online content

Any methods, additional references, Nature Research reporting summaries, source data, extended data, supplementary information, acknowledgements, peer review information; details of author contributions and competing interests; and statements of data and code availability are available at https://doi.org/10.1038/s41586-020-2137-8.

1. Schönherr, H. & Cernak, T. Profound methyl effects in drug discovery and a call for new C–H methylation reactions. *Angew. Chem. Int. Ed.* **52**, 12256–12267 (2013).
2. Cernak, T., Dykstra, K. D., Tyagarajan, S., Vachal, P. & Krska, S. W. The medicinal chemist's toolbox for late stage functionalization of drug-like molecules. *Chem. Soc. Rev.* **45**, 546–576 (2016); correction **46**, 1760 (2017).

3. Barreiro, E. J., Kümmerle, A. E. & Fraga, C. A. M. The methylation effect in medicinal chemistry. *Chem. Rev*. **111**, 5215–5246 (2011).
4. Leung, C. S., Leung, S. S. F., Tirado-Rives, J. & Jorgensen, W. L. Methyl effects on protein-ligand binding. *J. Med. Chem*. **55**, 4489–4500 (2012).
5. Fauber, B. P. et al. Discovery of 1-{4-[3-fluoro-4-((3S,6R)-3-methyl-1,1-dioxo-6-phenyl-[1,2] thiazinan-2-ylmethyl)-phenyl]-piperazin-1-yl}-ethanone (GNE-3500): a potent, selective, and orally bioavailable retinoic acid receptor-related orphan receptor c (RORc or RORγ) inverse agonist. *J. Med. Chem*. **58**, 5308–5322 (2015).
6. Quancard, J. et al. A potent and selective $S1P_1$ antagonist with efficacy in experimental autoimmune encephalomyelitis. *Chem. Biol*. **19**, 1142–1151 (2012).
7. Belshaw, P. J., Schoepfer, J. G., Liu, K.-Q., Morrison, K. L. & Schreiber, S. L. Rational design of orthogonal receptor-ligand combinations. *Angew. Chem. Int. Ed. Engl*. **34**, 2129–2132 (1995).
8. Shogren-Knaak, M. A., Alaimo, P. J. & Shokat, K. M. Recent advances in chemical approaches to the study of biological systems. *Annu. Rev. Cell Dev. Biol*. **17**, 405–433 (2001).
9. Blakemore, D. C. et al. Organic synthesis provides opportunities to transform drug discovery. *Nat. Chem*. **10**, 383–394 (2018).
10. White, M. C. & Zhao, J. Aliphatic C–H oxidations for late-stage functionalization. *J. Am. Chem. Soc*. **140**, 13988–14009 (2018).
11. Campos, K. R. Direct sp^3 C–H bond activation adjacent to nitrogen in heterocycles. *Chem. Soc. Rev*. **36**, 1069–1084 (2007).
12. Cordier, C. J., Lundgren, R. J. & Fu, G. C. Enantioconvergent cross-couplings of racemic alkylmetal reagents with unactivated secondary alkyl electrophiles: catalytic asymmetric Negishi α-alkylations of N-Boc-pyrrolidine. *J. Am. Chem. Soc*. **135**, 10946–10949 (2013).
13. Beak, P., Basu, A., Gallagher, D. J., Park, Y. S. & Thayumanavan, S. Regioselective, diastereoselective, and enantioselective lithiation-substitution sequences: reaction pathways and synthetic applications. *Acc. Chem. Res*. **29**, 552–560 (1996).
14. Milligan, J. A., Phelan, J. P., Badir, S. O. & Molander, G. A. Alkyl carbon-carbon bond formation by nickel/photoredox cross-coupling. *Angew. Chem. Int. Ed*. **58**, 6152–6163 (2019).
15. Paul, A. & Seidel, D. α-Functionalization of cyclic secondary amines: Lewis acid promoted addition of organometallics to transient imines. *J. Am. Chem. Soc*. **141**, 8778–8782 (2019).
16. Jain, P., Verma, P., Xia, G. & Yu, J.-Q. Enantioselective amine α-functionalization via palladium-catalysed C–H arylation of thioamides. *Nat. Chem*. **9**, 140–144 (2017).
17. Le, C., Liang, Y., Evans, R. W., Li, X. & MacMillan, D. W. C. Selective sp3 C–H alkylation via polarity-match-based cross-coupling. *Nature* **547**, 79–83 (2017).
18. Hiemstra, H. & Speckamp, W. N. in *Comprehensive Organic Synthesis: Selectivity, Strategy & Efficiency in Modern Organic Chemistry* **vol. 2** ch.4.5 (eds Trost, B. M. & Fleming, I.) 1047–1082 (Pergamon Press, 1991).
19. Li, Z., Bohle, D. S. & Li, C.-J. Cu-catalyzed cross-dehydrogenative coupling: a versatile strategy for C–C bond formations via the oxidative activation of sp^3 C–H bonds. *Proc. Natl Acad. Sci. USA* **103**, 8928–8933 (2006).
20. Andrus, M. B. & Lashley, J. C. Copper catalyzed allylic oxidation with peresters. *Tetrahedron* **58**, 845–866 (2002).
21. Kato, N., Hamaguchi, Y., Umezawa, N. & Higuchi, T. Efficient oxidation of ethers with pyridine N-oxide catalyzed by ruthenium porphyrins. *J. Porphyr. Phthalocyanines* **19**, 411–416 (2015).
22. Ito, R., Umezawa, N. & Higuchi, T. Unique oxidation reaction of amides with pyridine-N-oxide catalyzed by ruthenium porphyrin: direct oxidative conversion of N-acyl-L-proline to N-acyl-L-glutamate. *J. Am. Chem. Soc*. **127**, 834–835 (2005).
23. Yoshifuji, S., Tanaka, K.-I., Kawai, T. & Nitta, Y. Chemical conversion of cyclic α-amino acids to α-aminodicarboxylic acids by improved ruthenium tetroxide oxidation. *Chem. Pharm. Bull*. **33**, 5515–5521 (1985).
24. Kawamata, Y. et al. Scalable, electrochemical oxidation of unactivated C–H bonds. *J. Am. Chem. Soc*. **139**, 7448–7451 (2017).
25. Annese, C., D'Accolti, L., Fusco, C., Licini, G. & Zonta, C. Heterolytic (2e) vs homolytic (1e) oxidation reactivity: N–H versus C–H switch in the oxidation of lactams by dioxirans. *Chem. Eur. J*. **23**, 259–262 (2017).
26. Cui, L., Peng, Y. & Zhang, L. A two-step, formal [4+2] approach toward piperidin-4-ones via Au catalysis. *J. Am. Chem. Soc*. **131**, 8394–8395 (2009).
27. Zhao, J., Nanjo, T., de Lucca, E. C. & White, M. C. Chemoselective methylene oxidation in aromatic molecules. *Nat. Chem*. **11**, 213–221 (2019).
28. Chen, M. S. & White, M. C. Combined effects on selectivity in Fe-catalyzed methylene oxidation. *Science* **327**, 566–571 (2010).
29. Gormisky, P. E. & White, M. C. Catalyst-controlled aliphatic C–H oxidations with a predictive model for site-selectivity. *J. Am. Chem. Soc*. **135**, 14052–14055 (2013).
30. Osberger, T. J., Rogness, D. C., Kohrt, J. T., Stepan, A. F. & White, M. C. Oxidative diversification of amino acids and peptides by small-molecule iron catalysis. *Nature* **537**, 214–219 (2016).
31. Milan, M., Carboni, G., Salamone, M., Costas, M. & Bietti, M. Tuning selectivity in aliphatic C–H bond oxidation of N-alkylamides and phthalimides catalyzed by manganese complexes. *ACS Catal*. **7**, 5903–5911 (2017).
32. Nicolaou, K. C., Dolle, R. E., Chucholowski, A. & Randall, J. L. Reactions of glycosyl fluorides. Synthesis of C-glycosides. *J. Chem. Soc. Chem. Commun*. 1153–1154 (1984).
33. Posner, G. H. & Haines, S. R. Conversion of glycosyl fluorides into c-glycosides using organoaluminum reagents. Stereospecific alkylation at C-6 of a pyranose sugar. *Tetrahedron Lett*. **26**, 1823–1826 (1985).
34. Mason, J. D. & Weinreb, S. M. Total syntheses of the monoterpenoid indole alkaloids (±)-alstoscholarisine B and C. *Angew. Chem. Int. Ed*. **56**, 16674–16676 (2017).
35. Taylor, R. D., MacCoss, M. & Lawson, A. D. G. Rings in drugs. *J. Med. Chem*. **57**, 5845–5859 (2014).
36. Vitaku, E., Smith, D. T. & Njardarson, J. T. Analysis of the structural diversity, substitution patterns, and frequency of nitrogen heterocycles among U.S. FDA approved pharmaceuticals. *J. Med. Chem*. **57**, 10257–10274 (2014).
37. Stevens, R. V. Nucleophilic additions to tetrahydropyridinium salts. Applications to alkaloid syntheses. *Acc. Chem. Res*. **17**, 289–296 (1984).
38. Tomooka, K., Matsuzawa, K., Suzuki, K. & Tsuchihashi, G. I. Lactols in stereoselection 2. Stereoselective synthesis of disubstituted cyclic ethers. *Tetrahedron Lett*. **28**, 6339–6342 (1987).
39. Lunn, M. R. et al. Indoprofen upregulates the survival motor neuron protein through a cyclooxygenase-independent mechanism. *Chem. Biol*. **11**, 1489–1493 (2004).
40. Howell, J. M., Feng, K., Clark, J. R., Trzepkowski, L. J. & White, M. C. Remote oxidation of aliphatic C–H bonds in nitrogen-containing molecules. *J. Am. Chem. Soc*. **137**, 14590–14593 (2015).
41. Prendergast, M. A. et al. Central nicotinic receptor agonists ABT-418, ABT-089, and (–)-nicotine reduce distractibility in adult monkeys. *Psychopharmacology* **136**, 50–58 (1998).
42. Maryanoff, B. E. et al. Pyrroloisoquinoline antidepressants. Potent, enantioselective inhibition of tetrabenazine-induced ptosis and neuronal uptake of norepinephrine, dopamine, and serotonin. *J. Med. Chem*. **27**, 943–946 (1984).
43. Sugi, K. et al. Improved synthesis of paroxetine hydrochloride propan-2-ol solvate through one of metabolites in humans, and characterization of the solvate crystals. *Chem. Pharm. Bull*. **48**, 529–536 (2000).
44. Fujimoto, J. et al. Discovery of 3,5-diphenyl-4-methyl-1,3-oxazolidin-2-ones as novel, potent, and orally available Δ-5 desaturase (D5D) inhibitors. *J. Med. Chem*. **60**, 8963–8981 (2017).
45. Kitamura, M., Ohmori, K. & Suzuki, K. Divergent behavior of cobalt-complexed enyne having a leaving group. *Tetrahedron Lett*. **40**, 4563–4566 (1999).

Data availability

The data that support the findings of this study are available in the Supplementary Information and from the corresponding author upon reasonable request.

Acknowledgements Financial support for this work was provided by the National Institute of General Medical Sciences (NIGMS) Maximizing Investigators' Research Award (MIRA; grant R35 GM122525), and from Pfizer to study the modifications of natural products and medicinal compounds. We thank L. Zhu and the University of Illinois School of Chemical Science (SCS) nuclear magnetic resonance (NMR) laboratory for assistance with NMR spectroscopy, and B. Budaitis for checking the procedure in Fig. 3, molecule **8**. The Bruker 500-Mz NMR spectrometer was obtained with the financial support of the Roy J. Carver Charitable Trust, Muscatine, IA, USA.

Author contributions K.F. and R.E.Q. conducted the experiments and analysed the data. M.C.W., K.F. and R.E.Q. wrote the manuscript. M.C.W., K.F., R.E.Q., J.T.K., M.S.O. and U.R. designed the project. All authors provided comments on the experiments and manuscript during its preparation.

Competing interests The University of Illinois has filed a patent application (number 16/569,492) on the Mn(CF_3PDP) catalyst that lists M.C.W. as an inventor.

Additional information

Supplementary information is available for this paper at https://doi.org/10.1038/s41586-020-2137-8.

Correspondence and requests for materials should be addressed to M.C.W.

Extended Data Table 1 | Reaction optimization

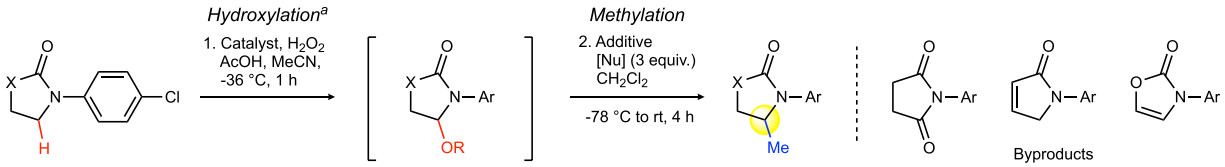

2, X = CH_2
S1, X = O
(1 equiv.)

4a (OH), R = H; **4a (OAc)**, R = Ac, X = CH_2
S2, R = H; **S3**, R = Ac, X = O

3, X = CH_2
7, X = O

4b **4c** **S4**

Entry	Substrate	Catalyst	Loading (mol %)	Additive	[Nu]	**4a (OH)**/ **S2** (%)	**4a (OAc)**/ **S3** (%)	**3**/**7** (%)	**4b** (%)	**4c**/**S4** (%)	rsm (%)
Oxidation											
1[b]	**2**	Fe(PDP)	3 x 5	—	—	< 5[k]	0	—	< 5[k]	—	0
2[c]	**2**	Fe(CF_3PDP)	3 x 5	—	—	8[k]	0	—	6[k]	—	0
3[d]	**2**	Mn(PDP)($OTf)_2$	1	—	—	12	0	—	0	—	75
4	**2**	Mn(PDP)($SbF_6)_2$	1	—	—	28	7	—	< 5[k]	—	35
5[e]	**2**	Mn(CF_3PDP) **1**	10	—	—	13[k]	10	—	41	—	0
6	**2**	**1**	1	—	—	51	21	—	9	—	0
7	**2**	**1**	0.5	—	—	64	18	—	< 5[k]	—	4
Methylation											
8[f]	**2**	**1**	0.5	BF_3•OEt_2	$AlMe_3$	< 5[k]	0	63	< 5[k]	0	11
9[f]	**S1**	**1**	0.5	BF_3•OEt_2	$AlMe_3$	11	5	10	—	4	27
10[g]	**S1**	**1**	0.5	DAST	$AlMe_3$	0	14[k]	55	—	0	16
11[g]	**2**	**1**	0.5	DAST	$AlMe_3$	0	0	64	< 5[k]	0	12
12[g]	**2**	**1**	0.5	Deoxo-Fluor	$AlMe_3$	0	0	61	6	0	5
13[h]	**2**	**1**	0.5	TFAA/ TMSOTf	$AlMe_3$	0	0	51	< 5[k]	14	9
14[h]	**S1**	**1**	0.5	TFAA/ TMSOTf	$AlMe_3$	0	0	46	—	20	13
15[i]	**2**	**1**	0.5	MsCl/NEt_3	$AlMe_3$	15	0	0	< 5[k]	39	6
16[g]	**2**	**1**	0.5	DAST	$ZnMe_2$	17	9	0	11	0	14
17[g,j]	**2**	**1**	0.5	DAST	MeMgBr	24	< 5[k]	24	< 5[k]	0	9

[a]General oxidation (unless otherwise noted): **2** (0.3 mmol), catalyst (x mol%, (*R*,*R*) and (*S*,*S*) enantiomers used interchangeably), AcOH (15 equiv.), MeCN (0.5 M), −36 °C; H_2O_2 (2 equiv.) in MeCN (3.75 ml) syringe pump 1 h. Mixture passed through silica plug, EtOAc flush, concentrated before isolation or methylation. Isolated yields are based on the average of three experiments, unless otherwise noted. [b]Procedure from ref. [28]. [c]Procedure from ref. [29]. [d]Procedure from ref. [31]. [e]5 equiv. H_2O_2. [f]General BF_3 alkylation: crude in CH_2Cl_2 (0.2 M), −78 °C, $AlMe_3$ (3 equiv.) and BF_3•OEt_2 (2 equiv.) sequentially added, stirred 1 h; room temperature (rt) for 3 h. [g]General fluorine alkylation: crude in CH_2Cl_2 (0.2 M), fluorine additive (1 equiv.) added at −78 °C; rt for 1 h; cooled to −78 °C, nucleophile (3 equiv.) added, stirred 2 h; rt for 1 h. [h]General TMSOTf alkylation: crude in CH_2Cl_2 (0.2 M), TFAA (1 equiv.) added, stirred 1 h; cooled to −78 °C, $AlMe_3$ (3 equiv.) and TMSOTf (1 equiv.) sequentially added, stirred 2 h; rt for 1 h. [i]Crude in CH_2Cl_2 (0.2 M), MsCl (1 equiv.) and Et_3N (1 equiv.) added, stirred 1 h; washed $NaHCO_3$, dried, reduced; redissolved in CH_2Cl_2, $AlMe_3$ (3 equiv.) added at −78 °C, stirred 2 h; rt for 1 h. [j]MeMgBr (3 equiv.) added at −78 °C, stirred 3 h. [k]Yield determined by crude ^{1}H-NMR.